



### Mycologia



ISSN: 0027-5514 (Print) 1557-2536 (Online) Journal homepage: www.tandfonline.com/journals/umyc20

## Pleoardoris graminearum, gen. et sp. nov., a new member of Pleosporales from North American Plains, its biogeography and effects on a foundation grass species

Xiomy-Janiria Pinchi-Davila, Diana Vargas-Hernández, María-José Romero-Jiménez, Ari Jumpponen, Jennifer A. Rudgers, Jose Herrera, Miriam Hutchinson, John M. Dunbar, Cheryl Kuske & Andrea Porras-Alfaro

**To cite this article:** Xiomy-Janiria Pinchi-Davila, Diana Vargas-Hernández, María-José Romero-Jiménez, Ari Jumpponen, Jennifer A. Rudgers, Jose Herrera, Miriam Hutchinson, John M. Dunbar, Cheryl Kuske & Andrea Porras-Alfaro (2023) *Pleoardoris graminearum*, gen. et sp. nov., a new member of Pleosporales from North American Plains, its biogeography and effects on a foundation grass species, Mycologia, 115:6, 749-767, DOI: 10.1080/00275514.2023.2258269

To link to this article: <a href="https://doi.org/10.1080/00275514.2023.2258269">https://doi.org/10.1080/00275514.2023.2258269</a>

+	View supplementary material 🗹
	Published online: 24 Oct 2023.
	Submit your article to this journal 🗷
ılıl	Article views: 353
a a	View related articles 🗷
CrossMark	View Crossmark data 🗗





# Pleoardoris graminearum, gen. et sp. nov., a new member of Pleosporales from North American Plains, its biogeography and effects on a foundation grass species

Xiomy-Janiria Pinchi-Davila o<sup>a</sup>, Diana Vargas-Hernández<sup>b</sup>, María-José Romero-Jiménez<sup>b</sup>, Ari Jumpponen<sup>c</sup>, Jennifer A. Rudgers<sup>d</sup>, Jose Herrera<sup>e</sup>, Miriam Hutchinson<sup>f</sup>, John M. Dunbar<sup>f</sup>, Cheryl Kuske<sup>f</sup>, and Andrea Porras-Alfaro<sup>g,h</sup>

<sup>a</sup>Department of Plant Pathology, University of Georgia, Athens, Georgia, 30602; <sup>b</sup>Department of Biological Sciences, Western Illinois University, Macomb, Illinois, 61455; <sup>c</sup>Division of Biology, Kansas State University, Manhattan, Kansas, 66506; <sup>d</sup>Department of Biology, University of New Mexico, Albuquerque, New Mexico, 87131; <sup>e</sup>Office of the Provost and Executive Vice President for Academic Affairs, University of Northern Iowa, Cedar Falls, Iowa, 50614; <sup>f</sup>Los Alamos National Laboratory, Los Alamos, New Mexico, 87545; <sup>g</sup>Institute for Environmental Studies, Western Illinois University, Macomb, Illinois, 61455; <sup>h</sup>Division of Environmental Biology, National Science Foundation, Alexandria, Virginia 22314

#### **ABSTRACT**

Diverse fungi colonize plant roots worldwide and include species from many orders of the phylum Ascomycota. These fungi include taxa with dark septate hyphae that colonize grass roots and may modulate plant responses to stress. We describe a novel group of fungal isolates and evaluate their effects on the grass Bouteloua gracilis in vitro. We isolated fungi from roots of six native grasses from 24 sites spanning replicated latitudinal gradients in the south-central US grasslands and characterized isolates phylogenetically using a genome analysis. We analyzed 14 isolates representing a novel clade within the family Montagnulaceae (order Pleosporales), here typified as *Pleoardoris graminearum*, closely related to the genera *Didymocrea* and *Bimuria*. This novel species produces asexual, light brown pycnidium-like conidioma, hyaline hyphae, and chlamydospores when cultured on quinoa and kiwicha agar. To evaluate its effects on B. gracilis, seeds were inoculated with one of three isolates (DS304, DS334, and DS1613) and incubated at 25 C for 20 d. We also tested the effect of volatile organic compounds (VOCs) produced by the same isolates on B. gracilis root and stem lengths. Isolates had variable effects on plant growth. One isolate increased B. gracilis root length up to 34% compared with uninoculated controls. VOCs produced by two isolates increased root and stem lengths (P < 0.05) compared with controls. Internal transcribed spacer ITS2 metabarcode data revealed that P. graminearum is distributed across a wide range of sites in North America (22 of 24 sites sampled), and its relative abundance is influenced by host species identity and latitude. Host species identity and site were the most important factors determining P. graminearum relative abundance in drought experiments at the Extreme Drought in the Grasslands Experiment (EDGE) sites. Variable responses of B. gracilis to inoculation highlight the potential importance of nonmycorrhizal root-associated fungi on plant survival in arid ecosystems.

#### **ARTICLE HISTORY**

Received 29 September 2022 Accepted 8 September 2023

#### **KEYWORDS**

Dark septate endophytes; drought; heat stress; latitudinal gradient; novel genus; Pleosporales; root-associated fungi; 2 new taxa

#### **INTRODUCTION**

Ongoing global environmental change includes warming air temperatures, greater drought intensity and frequency of extreme events, and increases in soil salinity, erosion, and eutrophication (Masson-Delmotte et al. 2018; Woodward et al. 2012). These environmental changes can alter the structure and composition of plant communities by reducing or eliminating foundation species, which stabilize conditions for other species and modulate fundamental ecosystem functions (Dayton 1972; Ellison et al. 2005; Emery and Rudgers 2013; Thomson et al. 2015). Symbiotic microorganisms, particularly dark septate root fungi (DSF; Ascomycota)

that colonize the roots of foundation plant species, have potential to enhance plant resistance to drought and heat (Mandyam and Jumpponen 2005). Despite this potential, surprisingly little is known about the diversity and ecology of these common root-associated fungi.

DSF are a diverse group of fungi that includes many orders within the phylum Ascomycota, such as Pleosporales, Helotiales, Sordariales, and Xylariales (Jumpponen and Trappe 1998). These fungi have melanized hyphae, form microsclerotia, and colonize the root epidermis and cortex typically without causing disease (Jumpponen 2001; Jumpponen and Trappe 1998; Knapp et al. 2012). DSF have been reported from more

than 600 plant species representing at least 100 families of angiosperms and gymnosperms (Mandyam and Jumpponen 2005). Some DSF can confer drought tolerance, enhance plant growth and biomass, increase disease resistance, or ameliorate abiotic stress (Kivlin et al. 2013; Li et al. 2018; Newsham 2011; Rodriguez et al. 2009; Santos et al. 2021; Woodward et al. 2012; Zhang et al. 2017).

DSF can also influence plant growth through the production of volatile organic compounds (VOCs). These compounds have low molecular mass and high vapor pressure, which allows them to evaporate and diffuse aboveground and belowground (Naznin et al. 2013; Schulz-Bohm et al. 2017). The effects of VOCs on plant growth are poorly understood; some studies suggest that they can play important roles in pollination, defense against herbivores, or act as biocontrols against other fungal pathogens (Berthelot et al. 2016; Hung et al. 2013). Although some studies have focused on the effect of VOCs produced by Trichoderma species (Hung et al. 2013; Lee et al. 2015) and other DSF (Naznin et al. 2013; Paul and Park 2013) in dicot plants, none have tested the effects of VOCs produced by DSF on foundation grass species.

Pleosporales is one of the most abundant orders of Ascomycota, with large numbers of DSF described from drylands. For instance, root fungal endophyte communities associated with the most widespread grass species in North American grassland ecosystems, Bouteloua gracilis (blue grama grass), are dominated by novel groups of DSF (Jumpponen et al. 2017; Porras-Alfaro et al. 2008; Rudgers et al. 2022). The large number of novel fungal clades described from dry grasslands suggests that these ecosystems represent important hot spots of DSF diversity, particularly for Pleosporales (Knapp et al. 2012; Porras-Alfaro et al. 2008). Yet, few studies have described these novel endophytic species or tested their interactions with plants. Analyses of DSF biogeography, and their interactions with plants under drought or other environmental stressors, may provide fundamental clues about the importance of root-associated endophytes to plant communities of the future (Jumpponen et al. 2017; Kivlin et al. 2013; Lagueux et al. 2021).

Here, we describe a new species of Pleosporales and report on its potential to influence the growth of Bouteloua gracilis. We also tested whether VOCs released by these fungi could stimulate host growth in the absence of direct inoculation and colonization of plant roots. We determined the biogeographic distribution of this novel fungal taxon in roots of six foundation grass species and tested for host specificity using internal transcribed spacer ITS2 metabarcode sequencing across replicated latitudinal gradients over central and

western North American grasslands (see survey details in Rudgers et al. 2022). Finally, we used a long-term drought experiment (Extreme Drought in the Grasslands Experiment [EDGE]) spanning six field sites that coincided with our latitudinal gradient to test whether drought altered the relative abundance of this new species in host roots.

#### **MATERIALS AND METHODS**

Site description and sample collection.— We examined fungal isolates from an established collection obtained from roots of five grass species: Andropogon gerardii (big bluestem, ANGE), B. dactyloides (buffalo grass, BUDA), B. eriopoda (black grama, BOER), B. gracilis (blue grama, BOGR), and Schizachyrium scoparium (little bluestem, SCSC), collected across 24 sites as part of a latitudinal survey in the North American Plains (SUPPLEMENTARY TABLE 1) (Rudgers et al. 2022). Briefly, 12 individuals per plant were sampled at each site at 10-m intervals along five transects spaced 10 m apart in a total area of 40 × 40 m sampling grid per species. At each site, we also collected a suite of geographic (longitude, latitude, elevation), climate (annual precipitation of 2015, average annual precipitation of 3 years, average annual precipitation of 30 years, soil gravimetric water content, growing degree days [GDDs for 2015, GDDs of 3 years, and GDDs of 30 years], plant trait (specific leaf area), and edaphic (pH, ammonium, soil organic matter, nitrate, and phosphorus) variables to compare their relative influence on fungal biogeography (details on methods in Rudgers et al. 2022).

Fungal isolation.—Fungi were isolated from surfacesterilized roots within 48 h of being collected in the field. We cut surface-sterilized roots into 2-3-mm sections and incubated six root fragments from each sampled plant at room temperature in a 48-well tissue culture plate (Fisher Scientific, Waltham, Massachusetts) with 2% malt extract agar (MEA) (Difco Laboratories, Sparks, Maryland) amended with antibiotics (streptomycin and tetracycline, 50 mg/L). Emerging colonies were transferred to Petri plates with MEA to obtain pure cultures. Over 1000 fungal isolates were recovered. The holotype specimen of the novel taxon was dried, and in the form of a biologically inert agar culture it was deposited in the fungarium of the Florida Museum of Natural History under the accession number FLAS-F-71013. Ex-type cultures were deposited at the University of New Mexico Fungarium (Rudgers, New Mexico) and Los Alamos National Laboratory (Los Alamos, New Mexico).

DNA extraction, PCR sequencing, and phylogenetic analysis.—We extracted genomic DNA from pure cultures using the DNeasy Plant Mini Kit (Qiagen, Valencia, California) and the Wizard genomic DNA purification kits (Promega, Madison, Wisconsin) following the manufacturers' instructions. We screened the culture collection using ITS sequencing (1033 isolates in total) and selected 14 isolates representing this potential novel taxon for further morphological characterization and sequencing of additional markers and phylogenetic analyses. Of these 14 isolates, four were obtained from roots of B. gracilis and two from B. dactyloides from Ladybird Johnson Wildlife Center (CAD), Texas; three from B. gracilis and three from B. eriopoda roots from Guadalupe Mountains National Park (GMT), Texas; one from B. gracilis roots from Spring Creek Audubon (SCP), Nebraska; and one from B. gracilis roots from Carson National Forest (CNF), New Mexico. A total of six loci were polymerase chain reaction (PCR)-amplified: sequences of ITS1-5.8S-ITS2 rDNA (ITS), partial nuc 28S rDNA (28S), and partial nuc 18S rDNA (18S) and partial gene sequences for calmodulin (CAL), actin (ACT), and  $\beta$ tubulin (TUB). We used primer pairs ITS1F (Gardes and Bruns 1993) and ITS4 (White et al. 1990) for the ITS region, LR0R (Rehner and Samuels 1994) and LR5 (Vilgalys and Hester 1990) for the partial nuc 28S nrRNA, NS1 and NS4 (White et al. 1990) for the partial nuc 18S nrRNA, ACT-512 F (Carbone and Kohn 1999) and ACT-2Rd (Quaedvlieg et al. 2011) for actin, CAL-228 F (Carbone and Kohn 1999) and CAL-2Rd (Groenewald et al. 2013) for calmodulin, and CYLTUB1F (Groenewald et al. 2013) and Bt-2b (Glass and Donaldson 1995) for β-tubulin. The PCR conditions for ITS consisted of 95 C for 5 min, followed by 35 cycles of denaturation at 94 C for 30s, annealing at 55 C for 30s, and elongation at 72 C for 45s, with a final extension step at 72 C for 7 min. The PCR conditions

for the partial nuc 18S nrRNA (18S) and 28S nrRNA (28S) consisted of 95 C for 5 min, followed by 35 cycles of denaturation at 94 C for 30s, annealing at 56 C for 30s, and elongation at 72 C for 45s, with a final extension step at 72 C for 7 min. The PCR conditions for CAL, ACT, and TUB consisted of 95 C for 5 min, followed by 35 cycles of denaturation at 95 C for 30s, annealing at 55 C for 30s, and elongation at 72 C for 40s, with a final extension step at 72 C for 5 min. We visualized PCR products with 1.2% agarose gel electrophoresis stained with GelRed (nucleic acid stain, Biotium, Fremont, California) in Tris-acetate-EDTA buffer (TAE, Edvotek, Washington, DC) and sequenced the PCR amplicons using the forward and reverse primer pairs at GENEWIZ (South Plainfield, New Jersey). Obtained sequences were assembled, trimmed, and edited using Sequencher 4.0 (Gene Codes, Ann Arbor, Michigan). Acquired sequence data were compared with the National Center for Biotechnology Information (NCBI) and UNITE databases using BLASTn following the cutoff for genus identification (Vu et al. 2019). Sequences are available at GenBank (TABLE 1). Due to the lack of representative sequences for closely related taxa for ITS and other genes, a singlegene 28S phylogeny was constructed to determine taxon placement. We also conducted a more detailed phylogenomic analysis using a larger number of genes and the closest relatives identified using BLASTn and 28S phylogenetic analysis (see below). For analysis of the 28S region, sequences were aligned in MEGA11 (Tamura et al. 2021) using MUSCLE. The 28S region contains the largest number of close relatives of our putative new taxon. Additionally, sequences for each gene were identified using GenBank (marker list) and UNITE (ITS), considering the taxon with the highest percentage of sequence similarity to be the closest relative. A phylogeny was inferred using the maximum likelihood method, and Tamura-Nei model with a discrete

Table 1. GenBank accession numbers of six different genes sequenced for P. graminearum isolates, collection site and plant host.

Isolate	Site code	Host	ITS	28S	185	ACT	CAL	TUB
DS168	CAD	BOGR	MK808530	MT707508	MT707482	MT750204	MT733186	
DS170	CAD	BOGR	MK808543	MT707509	MT707483	MT750205	MT733187	_
DS172	CAD	BOGR	MK808559	MT707510	MT707484	MT750206	MT733188	_
DS187	CAD	BOGR	MK808573	MT707511	MT707485	MT750207	MT733189	_
DS214	CAD	BUDA	MK808597	MT707512	MT707486	MT750208	MT733190	_
DS240	CAD	BUDA	MK808617	MT707513	MT707487	_	MT733191	_
DS304*	GMT	BOGR	MK808676	MT707514	MT707488	MT750209	MT733192	MW883074
DS328	GMT	BOER	MK808697	MT707515	MT707489	MT750211	MT733193	_
DS334	GMT	BOGR	MK808704	MT707516	MT707490	MT750210	MT733194	MW883075
DS338	GMT	BOGR	MK808707	MT707517	MT707491	MT750212	MT733195	_
DS342	GMT	BOER	MK808712	MT707518	MT707492	MT750213	MT733196	_
DS345	GMT	BOER	MK808715	MT707519	MT707493	MT750214	MT733197	_
DS1133	SCP	BOGR	MK808134	MT707520	MT707494	_	_	_
DS1613	CNF	BOGR	MK808482	MT707521	MT707495	MT750215	MT733198	MW883076

Note. BOGR = B. gracilis; BUDA = B. dactyloides; BOER = B. eriopoda. Site codes: CAD = Ladybird Johnson Wildlife Center, Texas; GMT = Guadalupe Mountains National Park, Texas; SCP = Spring Creek Audubon, Nebraska; CNF = Carson National Forest, New Mexico. \*Type species.

Gamma distribution was selected as the best model to infer the evolutionary distances between sites based on the Bayesian information criterion (BIC). The analysis included 31 nucleotide sequences with a total of 848 positions. Bootstrap confidence for the clades was estimated using 1000 replicates; values above 70% are presented. The phylogenetic tree was rooted with *Venturia populina* (Venturiaceae, Venturiales) as the outgroup. All analyses were conducted in MEGA11 (Tamura et al. 2021).

**Phylogenomic** analysis.—Genomic DNA extracted from isolates DS304 (holotype) and DS1316 as previously described in Romero-Jiménez et al. (2022). Libraries for isolate DS304 were prepared as described in Mueller et al. (2016), and these were added as a spike into three separate rrn gene 300-bp paired-end amplicon sequencing runs on an Illumina MiSeq platform (Beckman Coulter Genomics, Danvers, Massachusetts) in the same manner implemented by Torres-Cruz et al. (2017) to obtain the Bifiguratus adelaidae genome. Libraries for isolate DS1613 were prepared as for DS304 and spiked into two rrn gene amplicon sequencing runs. Further, one additional run was prepared with the Illumina NextSeq Mid-Output Kit and sequenced (300 cycles) on the Illumina NextSeq 550 using the procedure described in Albright et al. (2018) to produce 150-bp paired-end reads.

Raw reads were first filtered with BBTools using the BBDuk command (Bushnell et al. 2017) to remove any adapter or PhiX sequences. Settings were adjusted to specify a hamming distance of 2, a minimum Q-score of 10, and a minimum k-mer size of 8, and paired-end reads were trimmed to the same length. Next, pairedends were assembled with SPAdes 3.13.1 (Bankevich et al. 2012) at default k-mer settings, using the "careful" mode and the read-cutoff value set to "auto." The assembly was then further processed with AAFTF 0.2.3 (Automated Assembly for the Fungi; Stajich and Palmer 2018) using default parameters. Briefly, scaffolds were scanned for vector sequences with the "vecscreen" command, followed by identification and removal of reads from contaminant organisms with the "sourpurge" command. Finally, duplicate contigs were dropped from the assembly using the "rmdup" command, and the genome was polished with five rounds of Pilon (Walker et al. 2014) to fill gaps and correct errors. Genes were predicted for the assemblies of each isolate using the FUNANNOTATE 1.8.1 pipeline (Love et al. 2018), implementing both AUGUSTUS 3.2.1 (Stanke et al. 2004) and GeneMark-ES 4.62 (Ter-Hovhannisyan et al. 2008) ab initio predictors. Genome completeness was determined with BUSCO (Benchmarking Universal Single-Copy Orthologs) 4.0.5 (Simão et al. 2015), using "pleosporales\_odb10" as the lineage data set, and default settings. Genome quality was determined with QUAST (Quality Assessment Tool for Genome Assemblies) 5.0.2 (Gurevich et al. 2013). Nucleotide content and structure was assessed with OcculterCut (Testa et al. 2016). Using the "compare" command in FUNANNOTATE (Love et al. 2018), a RAxML (Stamatakis 2014) phylogeny was compiled from 500 concatenated single-copy orthologs identified by BUSCO analysis. Regions were aligned using MAFFT (Katoh and Standley 2013). and the PROTGAMMAAUTO substitution model was employed with 1000 rapid replicates for bootstrapping. The resulting tree was visualized in FigTree 1.4.4 (Rambaut and Drummond 2012). Genomes of our two isolates, DS304 and DS1613, were compared with genomes of other pleosporalean isolates existing in public repositories at the Joint Genome Institute (JGI) and NCBI: two isolates in Lentitheciaceae, three isolates in Massarinaceae, and four isolates in Montagnulaceae. Trematosphaeria pertusa (Trematosphaeriaceae, Pleosporales) isolate CBS 122368 served as the outgroup for rooting the phylogeny. This Whole Genome Shotgun project for DS304 and DS1613 has been deposited at DNA DataBank of Japan (DDBJ)/European Nucleotide Archive (ENA)/ GenBank under the accession JASMNA000000000. Information on the isolates that were used is provided in SUPPLEMENTARY TABLE 2.

**Morphological characterization.**—We excised mycelium plugs (5 mm diam) from all isolates and cultured them in seven different media: 2% malt extract agar (MEA) (Difco Laboratories, Sparks, Maryland), potato dextrose agar (PDA) (Oxoid, Hampshire, England), dichloran-glycerol (DG18) agar (Oxoid), Czapek-Dox agar (CDA) (Fluka Analytical, Buchs, Switzerland), oatmeal agar (OA), quinoa agar (QN), and kiwicha agar (KW). Media were prepared following the manufacturers' instructions. We prepared oatmeal agar using oatmeal flakes, whereas quinoa agar and kiwicha agar were prepared using quinoa (Cusco, Peru) and kiwicha (Cusco) flour. Approximately 100 g/L of each flour was dissolved, boiled for 20 min, and filtered with gauze. Finally, 15 g/L of agar was added. All media were autoclaved at 121 C for 20 min. We used oatmeal, quinoa, and kiwicha agar to induce sporulation (Bustamante Gonzales 2018), cultures were incubated in darkness and evaluated every 2 d for 2 months, and a 6210 RAL Chart K7-2014 (Elcometer, Warren, Michigan) was used

to describe standard colors of the colonies. Other methods were tested to promote sporulation, including the use of near-ultraviolet light and plant material as described in Knapp et al. (2015). However, they did not induce sporulation in any of our isolates, and we do not further discuss those results in this paper.

Additionally, we conducted physiological and chemical tests, and plant interaction assays (described in the corresponding section) for the holotype culture (DS304) and two additional cultures (DS334 and DS1613). We cultured mycelium blocks on modified Melin-Norkrans agar (MMN) (Plantmedia, Dublin, Ohio) Sabouraud dextrose agar (SDA) (Oxoid), soil agar (SA) (Himedia, West Chester, Pennsylvania), synthetic nutrient-poor agar (SNA) (Mueller et al. 2004), and Leonian's agar (LA) (Mueller et al. 2004) to promote spore production. Media were prepared following Mueller et al. (2004). Cultures were incubated at room temperature in darkness for 15 d.

**Physiological and chemical tests.**—Because these fungi colonize roots of plants living in arid ecosystems where drought and high salinity are major abiotic stressors, isolates DS304, DS334, DS1613 were tested in three levels of salt concentrations to measure their drought-osmotic tolerance induced by salt stress following protocols described in Mueller et al. (2004). Briefly, isolates were cultured on 10 cm Petri Petri dishes divided in four, each section containing MEA amended with different NaCl concentrations (0, 50, 100, and 150 g/L). Cultures were incubated in darkness for 15 d at room temperature. We considered our isolates salt tolerant if any growth was observed in the 50, 100, or 150 g/L NaCl treatment.

We also evaluated the amylolytic, cellulolytic, and proteolytic activities as described in Tamayo-Londoño (2017) to have a better understanding of the potential ecological roles of DSF and their ability to access nutrients from the host plant. We prepared the amylolytic assay medium using starch (2 g/L), peptone (1 g/L), yeast extract (1 g/L), and agar (20 g/L). The cellulolytic activity assay medium was prepared using carboxymethylcellulose (10 g/L), ammonium sulfate (5 g/L), K<sub>2</sub>HPO<sub>4</sub> (1 g/L), CaCl<sub>2</sub>·2H<sub>2</sub>O (0.01 g/L), MgSO<sub>4</sub>·7H<sub>2</sub>O (0.5 g/L), yeast extract (0.5 g/L), and agar (15 g/L). The proteolytic activity assay medium was prepared using nutritive agar supplemented with Knox unflavored gelatine (0.4%, the jelly solution is sterilized separately from the nutritive agar and added as 50 mL/L; Kraft Heinz Foods Company, Chicago, Illinois). All media were autoclaved at 121 C for 15 min and poured on small Petri dishes. We transferred mycelium blocks (1 cm<sup>2</sup>) to the center of the Petri dish and incubated in darkness for 8 d at room temperature. To test the amylolytic activity, we added an aqueous solution of Lugol's iodine in water (2:1 v/v) to the Petri dish; the test was considered positive if a yellow halo appeared around the colony and negative if the medium remained blue. We determined the cellulolytic activity by adding Congo red (2%) for 15 min to Petri dishes, which were then washed with distilled water and flooded with 1 M NaCl for 15 min. The cellulolytic activity was positive if the medium color changed from red to yellow-orange and negative if it remained red. We determined the proteolytic activity by flooding the Petri dishes in a saturated solution of ammonium sulfate for 15 min. The test was considered positive if a clear halo appeared around the colony and negative if the medium remained opaque.

Microscopy.—We prepared permanent slides using the microculture technique (Riddell 1950). Sterile slides and coverslips were placed in a sterile Petri dish, and and two 1 cm<sup>2</sup> medium blocks of malt extract, kiwicha, quinoa, and oatmeal agar were placed on the slide. We placed fungal tissue on each side of the blocks using an inoculation needle, and the coverslips were placed on top of each block. Finally, a moist sterile cotton ball was placed inside each Petri dish to maintain humidity. Microcultures were incubated at room temperature in darkness for 7 d, then under black light for 24 h, and returned to darkness for 30 d (Leach 1962). We removed the coverslips from the mycelium blocks and placed them on clean slides containing a drop of lactophenol blue. We observed the morphological structures using a light microscope with a camera included (Leica Microsystems DM1000; Buffalo Grove, Illinois).

**Plant interaction assays.**—Three fungal isolates (DS304, DS334, and DS1613) were tested to evaluate their effects on B. gracilis growth. This native grass is widely distributed in the North American Plains and was selected because of its relatively higher germination rates compared with the other grasses that were also sampled in Rudgers et al. (2022). We aseptically transferred three mycelial plugs (5 mm diam) from the edge of a growing colony on MEA to a 50 mL Falcon tube containing 35 mL of malt extract broth (17 g/L). The liquid culture was incubated at room temperature on an orbital shaker at 160 rpm for 14 d. After the incubation, we collected the fungal tissue by decanting and suspended it in distilled water (approx. 1 cm<sup>2</sup> mycelium clumps in 4 mL water). Bouteloua gracilis seeds were placed on Petri dishes containing 210 g of sterilized sand (30 seeds per plate  $\times$  3 Petri dishes [served as blocks]  $\times$  4

treatments [3 isolates plus a negative control], which means a total of 360 seeds, 10% [w/v] of water content). We inoculated treatment plates with 3 mL of fungal suspensions; 3 mL of distilled water was added to control plates. The Petri dishes were placed inside of a hinged, transparent plastic container ( $15 \times 15$  cm) to reduce cross-contamination. All plates were incubated in darkness for 2 d at room temperature and transferred into the growth chamber for 18 additional days with a diurnal photoperiod of 12 h of light/darkness at 25 C. We harvested seedlings on day 20 and measured the root and stem lengths. Root length was defined as the longest root measured without considering the lateral roots (Becker et al. 2016; Ndinga-Muniania et al. 2021).

We used the same fungal isolates (DS304, DS334, DS1613) to also test the effect of volatile organic compounds (VOCs) on B. gracilis growth. Fungal cultures were grown in small plastic Petri dishes containing MEA with chloramphenicol (50 mg/L) and incubated for 20 d at room temperature. Large glass Petri dishes were filled with sand, autoclaved twice at 121 C for 15 min, and dried for 50 min in an (Excalibur Dehydrators, Sacramento, California) food dehydrator. A total of seven 5-mm holes were drilled in the lid of the small plastic Petri dishes (6 cm diam), where fungi were grown, for gas exchange and the small plastic Petri dishes placed inside the larger glass Petri dishes (10 cm diam). We planted 30 seeds of B. gracilis around the small culture plate and added 10% (w/v) of water content. Our design included a total of 360 seeds (3 large Petri dishes [served as blocks] × 30 seeds × 4 treatments). Control plates did not contain any live inoculum but included a small plastic Petri dish with MEA. Our multiplate system (small Petri dish inside the larger Petri dish) was placed inside of a plastic PhytoCon (Phytotech Labs, Lenexa, Kansas) to limit gas exchange among treatments and reduce cross-contamination. We incubated all plates in darkness for 2 d at room temperature and transferred into the growth chamber for 18 additional days with a diurnal photoperiod of 12 h of light/darkness at 25 C. Seedlings were harvested by day 20, and the root and stem lengths were measured following the same criteria mentioned before. We used linear mixed models to test the effect of isolates on stem and root lengths. Models included the main effect of treatment and block as a random effect (R package LMER 1.2.5033). We performed post hoc pairwise comparisons of group means using estimated marginal means, using the Tukey method to correct for multiple comparisons (R package EMMEANS 1.2.5033).

We performed an additional test to evaluate the effects of the fungus on root morphology using surface-sterilized *B. gracilis* seeds inoculated with isolates DS304 and DS334. We sterilized *B. gracilis* seeds by soaking them

in 70% ethanol for 5 min, then seeds were submerged in 2% sodium hypochlorite solution for 20 min and washed three times with sterile distilled water. We incubated seeds on Petri dishes containing MEA supplemented with chloramphenicol (50 mg/L) for 2 d in darkness at room temperature and transferred them into the growth chamber for 2 additional days with a diurnal photoperiod of 12 h of light/darkness at 25 C. We selected fungus-free seeds and transferred them into glass tubes containing 15 mL of MMN medium and inoculated them with liquid inoculum of the fungus except for the controls (eight replicates per treatment). Tubes were sealed and incubated in the growth chamber for 35 d with a diurnal photoperiod of 12 h of light/darkness at 25 C. After incubation, we harvested seedlings and evaluated the length and color of the roots.

**Next-generation sequencing data sets.**—We extracted ITS sequences of this new fungal lineage from two large Illumina data sets obtained from the root samples analyzed in the latitudinal survey (mentioned in "Site description and sample collection") and the Extreme Drought in the Grasslands Experiment (EDGE) reported by Rudgers et al. (2022) and Lagueux et al. (2021), respectively. Briefly, the EDGE experiment includes six grassland sites spanning the central United States: the Central Plains Experimental Range (CPR), Hays Agricultural Research Center (HAR, grazed until 2012), High Plains Grassland Research Center (HPG, grazed until 2013), Konza Prairie (KNZ), and Sevilleta National Wildlife Refuge (SEVB, SEVG) (see survey details in Lagueux et al. 2021). Control and drought plots were arranged in 10 spatial blocks at each site, each block containing one ambient control and one drought plot. Treatments were applied to each block as described in Lagueux et al. (2021). Roots from six grass species, A. gerardii (ANGE), B. curtipendula (BOCU), B. eriopoda (BOER), B. gracilis (BOER), B. dactyloides (BUDA), and S. scoparium (SCSC), at each site were collected for Illumina sequencing. Prior to sequencing, we extracted total genomic DNA from ~20 1-cm root pieces per plant using MoBio PowerSoil DNA isolation kits (Carlsbad, California) and stored the DNA at -20 C until PCR amplification. Extracts were quantified and standardized to 1 ng/µL for PCR as described by Rudgers et al. (2022). We targeted the ITS2 region for PCR amplification using primers fITS7 (Ihrmark et al. 2012) and ITS4 (White et al. 1990). PCR cycles consisted of 98 C for 30s, followed by 35 cycles of denaturing at 98 C for 10s, annealing at 56 C for 10s, and extension at 72 C for 60s, and a final extension at 72 C for 5 min. Duplicate amplicons were processed, cleaned, and quantified as described by Lagueux et al.

(2021) and Rudgers et al. (2022). Data were rarefied to 10 000 reads per individual plant to avoid biases and to normalize data (Gihring et al. 2012; Lagueux et al. 2021; Rudgers et al. 2022).

To determine how edaphic and climate variables affect relative abundance of the newly described fungal species in the latitudinal survey, we assessed six edaphic variables at each of the 24 sites: soil ammonium (NH4<sup>+</sup>), nitrate (NO<sub>3</sub><sup>-</sup>), phosphorous (total P), pH, soil organic matter (SOM), and soil gravimetric water content (GWC). The climate data were obtained at 800 m spatial resolution from PRISM. We used linear mixed-effects models to test the significance of latitude and longitude on the distribution and relative abundance of the new fungal lineage. Models included the main effects of plant host, latitude, and their interaction as fixed effects, and collection site and replicated site gradient (west, mid, east) as random effects. Data were natural-log transformed (ln(X + 1)) to meet the assumptions for normality of residuals and homoscedasticity of variances. The analyses were repeated for longitude, plant traits, and edaphic or climate variables instead of latitude to explore the geographic distribution, host association, and environmental factors that correlate with the relative abundance of the new fungal lineage (R package LMER 1.2.5033). We ranked models for each predictor variable using the second-order Akaike's information criterion (AICc) (R package MUMLN 1.43.6) (Barton 2019) and calculated marginal R<sup>2</sup> (Lefcheck 2016; R package PIECEWISESEM 1.2.5033). Heatmaps were constructed using R packages GGPLOT2 3.2.1 (Wickham 2016) and GGMAP 3.0.0 (Kahle and Wickham 2013).

For the EDGE experiment, data were natural-log transformed (ln(X + 1)) to meet assumptions for normality of residuals and homoscedasticity of variances. We used a generalized linear model to test how the relative abundance of the fungus was affected by experimental drought depending on the site and host species combination (R package STATS 2.5033). We were unable to test plant and site effects separately because not all plant species were present in all EDGE sites. We also calculated the average effect of experimental drought over all sites and plant species and determined whether there were any significant differences between experimental drought and control plots depending on each site/species combination (R package EMMEANS 1.2.5033).

#### **RESULTS**

Sequence similarity, phylogenetics, and **phylogenomics.**—The closest relatives of these novel species based on BLASTn of the 28S region were Didymocrea sadasivanii CBS 438.65 (DQ384103, 98.5% identity), Neokalmusia kummingensis (NG068857, type, 98% identity), Kalmusia brevispora CBS 120248 (JX681110, 98% identity), and a number of sequences from soil and root environmental samples. For ITS, the majority of closely related sequences are from environmental samples or culture isolates with limited taxonomic information. A two-sequence alignment for ITS sequences using Didymocrea sadasivanii (MH870299) and Neokalmusia kummingensis (NR\_168208) showed no similarity when applying the default of highly similar sequences (megaBLAST), and lower than 72% similarity when optimized to somewhat similar sequences (BLASTn). Our 28S phylogeny showed that all 14 isolates clustered in a well-supported single clade (99% bootstrap support) closely related to Kalmusia scabrispora (AB524593), Neokalmusia kunmingensis (NG068857), and Didymocrea sadasivanii (CBS 438.65) and D. leucaenae (NG066304) (SUPPLEMENTARY FIG. 1). Our phylogenomic analysis is consistent with the 28S phylogeny and confirmed that isolates DS304 and DS1613 clustered in a single wellsupported clade distinct from Didymocrea sadasivanii (CBS 438.65) within the family Montagnulaceae in the order Pleosporales (FIG. 1). Thus, we propose the novel taxon Pleoardoris graminearum, gen. et sp. nov.

**Geographic distribution.**—The relative abundance of P. graminearum was structured biogeographically. Our Illumina sequencing detected P. graminearum in 22 of the 24 sites sampled. The relative distribution of P. graminearum significantly declined at higher latitudes consistently across host plant species (P < 0.05; latitude  $\times$  host species, P < 0.001; FIG. 2), whereas longitude did not influence the relative abundance of P. graminearun in a consistent way across plant species (P > 0.05). However, the interaction between longitude and host species identity (longitude × host species) predicted significantly the relative abundance of P. graminearum (P < 0.001). Specifically, in A. gerardii roots, P. graminearum was least abundant in western sites, whereas in other host species the relationship with longitude was weaker (B. dactyloides and B. gracilis) or neutral (S. scoparium). Bouteloua eriopoda could not be evaluated for an influence of longitude because it only occurred on the westernmost latitudinal gradient. Longitudinal trends in the relative abundance of Pleoardoris graminearum differed significantly between B. dactyloides and both S. scoparium and B. gracilis. The western and central sites had the greatest relative sequence abundance, with 25% (27 950 sequences) of the relative abundance in west

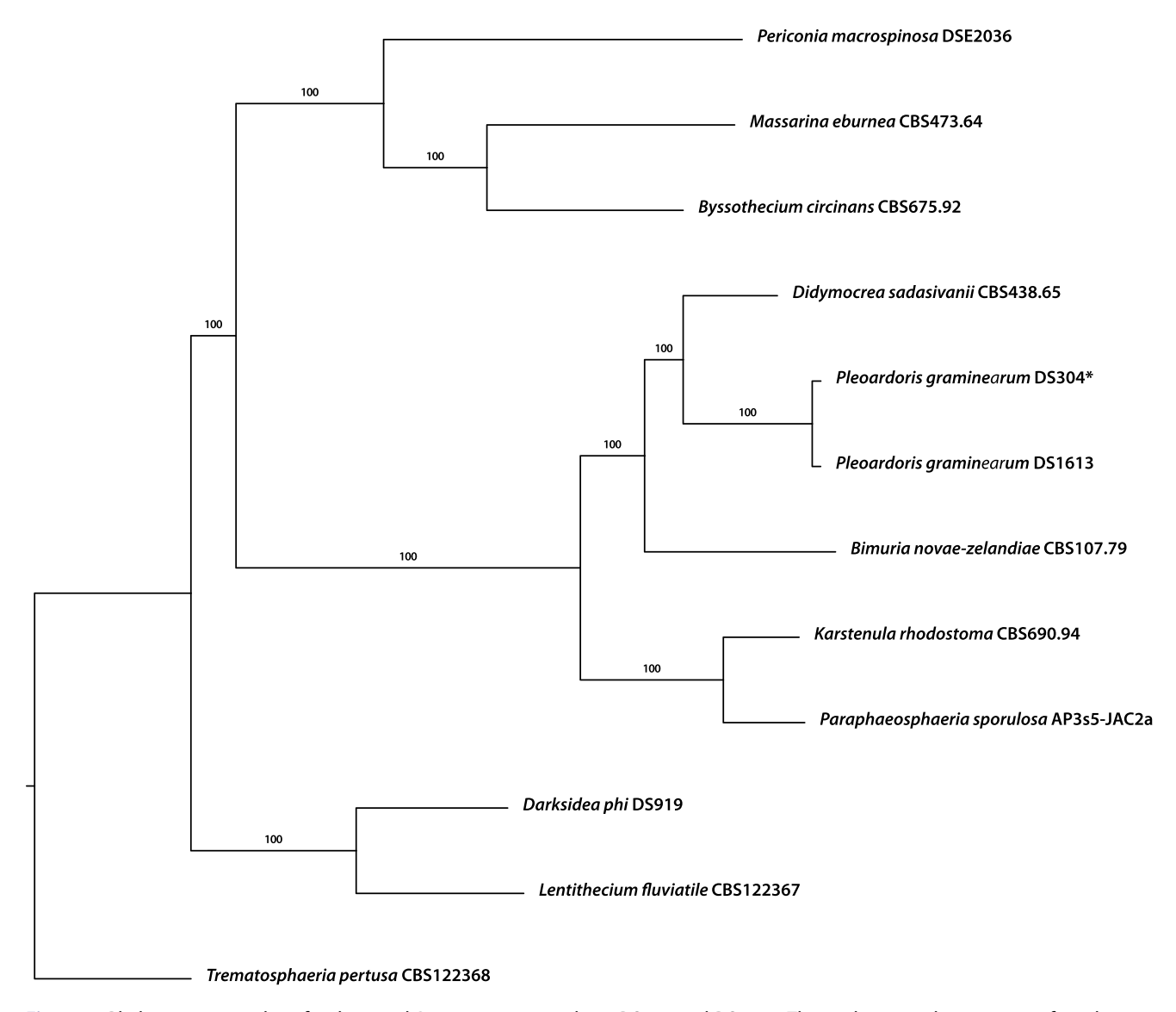


**Figure 1.** Phylogenomic analysis for the novel *P. graminearum* isolates DS304 and DS1613. The evolutionary history was inferred using the PROTGAMMAAUTO substitution model with 1000 rapid replicates for bootstrapping. *Trematosphaeria pertusa* isolate CBS 122368 served as the outgroup. \* denotes type species.

Texas (DMT) and 12% (13 814 sequences) in Ladybird Johnson Wildlife Center, Texas (CAD). In addition, *P. graminearum* was least abundant in Oklahoma (KAE, 6 sequences) and Nebraska (LAR, 1 sequence), and no sequences for this fungus were detected in Central Plains Experimental Range (CPR) or Konza Prairie (KNZ).

**Host association.**—Host species identity was an important factor in the geographic distribution of P. graminearum (P < 0.001; FIG. 3). Pleoardoris graminearum was most abundant in roots of B. gracilis (53 687 sequences) and B. eriopoda (28 951 sequences), followed by S. scoparium (12 291 sequences), B.

dactyloides (10 553 sequences), and A. gerardii (8142 sequences). Within a grass species, westernmost sites had the greatest abundance and number of sequences compared with easternmost sites (P > 0.05).

**Environmental correlates.**—Soil total phosphorus (AICc = 2487.8; TABLES 2 and 3) was the best correlate of P. graminearum relative abundance (marginal  $R^2$  = 0.26) and explained the most (26%) variation in its abundance. The relative sequence abundance of P. graminearum in A. gerardii, B. eriopoda, and S. scoparium roots was greatest in soils with low phosphorus soil content. This relationship with phosphorus was strongest in B. gracilis, followed by B. dactyloides. Pleoardoris

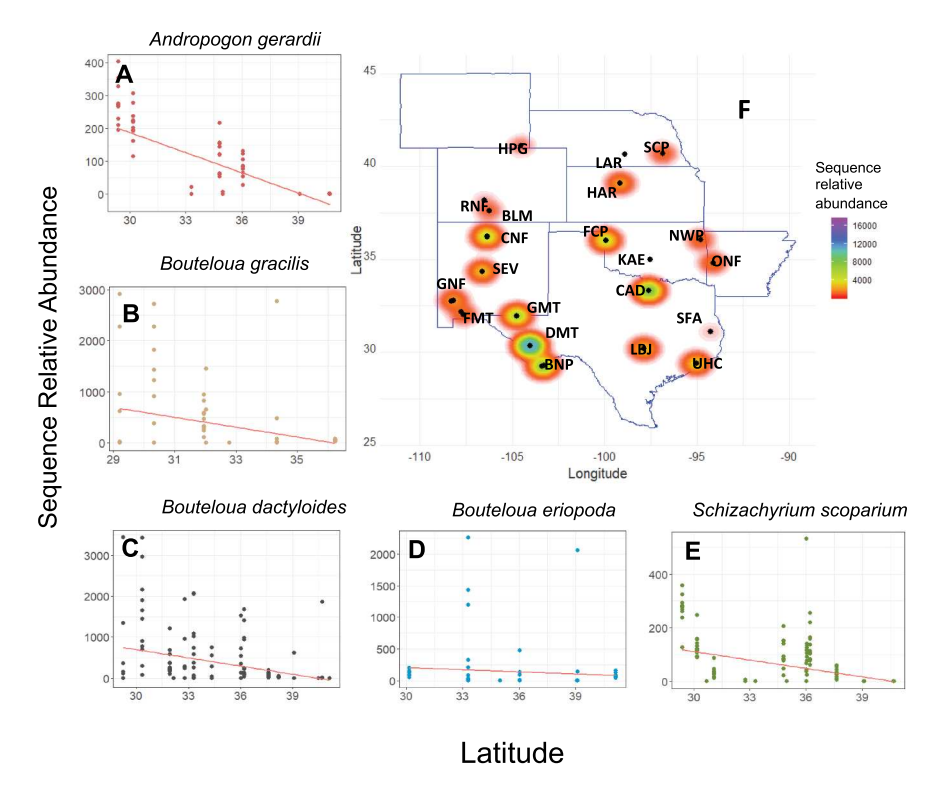


Figure 2. Relationship between P. graminearum relative abundance and latitude for each of five grass species. A. Andropogon gerardii. B. Bouteloua gracilis. C. Bouteloua dactyloides. D. Bouteloua eriopoda. E. Schizachyrium scoparium. F. Heat map showing Pleoardoris graminearum abundance and distributions along sampling sites. Color key shows sequence abundance: reddish colors represent low abundance; bluish/purplish represents higher abundance. Refer to SUPPLEMENTARY TABLE 1.

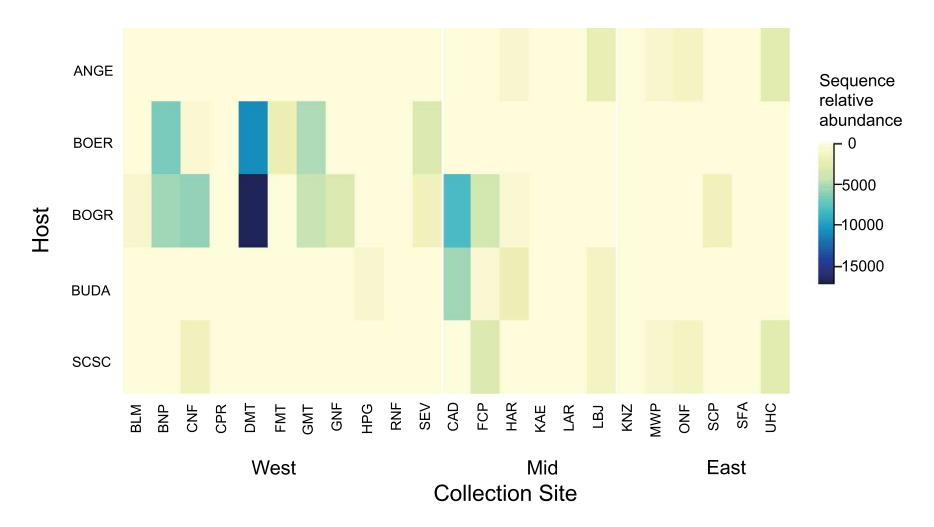


Figure 3. Heat map showing sequence relative abundance by site for the five grass species. Dark colors represent higher abundance; lighter colors show low abundance. ANGE = Andropogon gerardii; BOER = Bouteloua eriopoda; BOGR = Bouteloua gracilis; BUDA = Bouteloua dactyloides; CSC = Schizachyrium scoparium.

graminearum relative abundance significantly differed in phosphorus trends between B. gracilis and both A. gerardii and S. scoparium (SUPPLEMENTARY FIG. 2). The second-best correlate was latitude, followed by soil gravimetric soil water content, growing degree days, and soil ammonium (TABLE 2). Models that included the average soil pH and mean annual precipitation ranked last based on the AICc model selection criterion. However, whereas soil pH correlated with P. graminearum relative abundance (P < 0.05, pH marginal  $R^2 = 0.13$ ), precipitation did not (P > 0.05, precipitation marginal  $R^2 = 0.37$ ).

Table 2. Analysis of best correlates to determine P. graminearum relative abundance.

Environmental correlate	$R^2$	AICc
Soil phosphorus	0.26	2487.848
Latitude	0.30	2506.159
GWC	0.22	2506.893
GDD30Y	0.32	2512.085
Soil ammonium	0.21	2512.350
Soil nitrate	0.21	2512.350
PPT2015	0.45	2515.457
Soil moisture	0.21	2520.257
GDD3Y	0.23	2526.026
GDD2015	0.23	2528.466
SOM	0.26	2541.334
Foliar herbivory	0.11	2543.100
SLA	0.11	2544.527
PPT30Y	0.43	2545.314
Elevation	0.38	2546.116
Longitude	0.15	2557.285
PPT3Y	0.37	2558.898
Soil pH	0.13	2587.811

Note. Correlates are ranked in order of importance using the Akaike's information criterion (AICc); marginal  $R^2$  and P-values are given for each model. Edaphic correlates: soil ammonium (NH<sub>4</sub><sup>+</sup>), soil nitrate (NO<sub>3</sub><sup>-</sup>), soil phosphorus, soil pH, and soil organic matter (SOM). Climatic correlates: growing degree days (GDD3Y, GDD2015, and GDD30Y), annual precipitation (PPT3Y, PPT2015, PPT30Y), gravimetric water content (GWC), and average soil moisture. Geographic correlates: latitude, longitude, and elevation. Plant traits: specific leaf area (SLA) and foliar herbivory.

**Table 3.** Analysis of deviance of model including phosphorus, with site as random effect and plant species as fixed effect.

	•	
df	$\chi^2$	Р
1	24.017	< 0.0001
4	65.794	< 0.0001
1	21.143	< 0.0001
4	60.283	< 0.0001
4	60.077	< 0.0001
	df 1 4 1 4 4 4	4 65.794 1 21.143 4 60.283

**EDGE experiment.**—Experimental extreme drought did not affect the relative abundance of P. graminearum on average across host species or sites (treatment, P > 0.05; SUPPLEMENTARY FIG. 3). However, when we tested the effect of drought by site, P. graminearum relative abundance decreased in five of the six sites, by 22% to 69%. Drought effects also varied among host plant species (drought  $\times$  host species, P = 0.01). The relative abundance declined most with drought in B. gracilis and B. eriopoda at the Sevilleta National Wildlife Refuge in central New Mexico (SEVB, P < 0.05; SUPPLEMENTARY FIG. 3). In contrast, its relative abundance increased by 7% in drought treatments in B. curtipendula in Hays Agricultural Research Center in Kansas (HAR).

**Plant interaction assays.**—Fungal isolates had different effects on plant growth that ranged from negative to neutral or positive. For example, B. gracilis inoculated with isolates DS304, DS334, and DS1613 did not differ significantly from uninoculated controls in either root or stem length (P > 0.05; FIG. 4A). However, DS334 increased root length, up to 34% compared with controls. In contrast, B. gracilis plants in the VOC experiment treated with isolates DS304 and DS334 had significantly greater root and stem lengths than the controls (P < 0.05; FIG. 4B). The root systems inoculated with isolates DS304 and DS334 also differed morphologically from controls, with shorter and darkly pigmented roots following inoculation (FIG. 5).

#### **TAXONOMY**

Pleoardoris X.J. Pinchi-Davila & A. Porras-Alfaro, gen. nov. FIGS. 6-7; SUPPLEMENTARY FIG. 4 MycoBank MB836052

Typification: Pleoardoris graminearum X.J. Pinchi-Davila & A. Porras-Alfaro.

Etymology: From the Latin "ardoris," in reference to the distribution of the type species, mainly found in arid and semiarid lands, and "Pleo," in reference to the order Pleosporales.

Diagnosis: In addition to the phylogenetic, phylogenomic, and sequence similarity distinctions (FIG. 1; SUPPLEMENTARY FIG. 1), Pleoardoris is morphologically different from Didymocrea, Bimuria, and Kalmusia by the lack of sexual reproductive structures in culture and other asexual characteristics described below. In contrast to Pleordoris, Bimuria produces 2- or 3-spored asci, Didymocrea produces unitunicate asci and 2-celled spores, and Kalmusia forms ascomata with pigmented, verrucose ascospores. Additionally, Didymocrea and Bimuria were isolated from soils and Kalmusia from stem cortex cells, whereas *Pleoardoris* was isolated from roots.

Description: Isolates vary in color and mycelium morphology depending on the medium. Colonies on MEA, PDA, MMN, SDA, SNA, SA, OA+A, KW+A, and QN+A (antibiotic-amended OA, KW, and QN) vary from light ivory (RAL1015) to pearl (RAL1013), present radial growth with filamentous margins and flat or sparse aerial mycelium, sometimes with exudates. Colonies on Czapek-Dox agar vary from dark olivaceous to pearl (RAL1013), present branched growth with filamentous margins and flat mycelium, whereas colonies on DG18 vary from dark brown to light ivory (RAL1015), present radial growth with filamentous margins and flat mycelium. All cultures become darker (RAL1011, brown beige) in color or produce copper brown exudates (RAL 8004) after 30 d of incubation. On MEA, all isolates have mycelium composed of septate, highly branched, multinucleate, cylindrical, thin-walled hyphae, 1.4-4.2 µm diam, and  $2.6 \pm 0.7 \, \mu m$  average  $\pm$  SD (n = 30). Some cells in

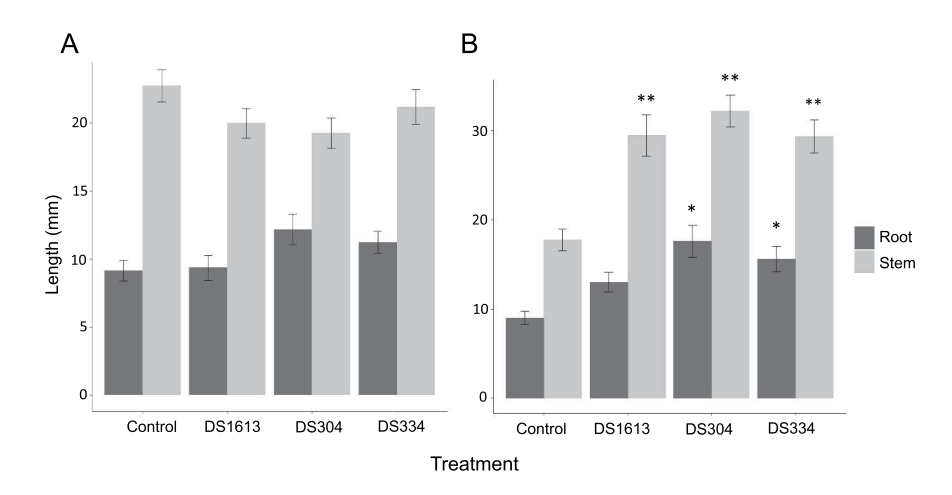


**Figure 4.** Effect of *P. graminearum* on *B. gracilis* growth after 20 d of incubation. A. Direct contact assay. B. Volatile organic compound (VOC) assay. Bar color groups measured variable. Bars represent mean  $\pm$  standard error. \* and \*\* denote significant differences between treatment and control.

hyphae are clavate or swollen, 6– $11.7 \times 3.8$ – $10.3 \, \mu m$  total range,  $8.6 \pm 1.7 \times 6.5 \pm 1.8 \, \mu m$  average  $\pm$  SD (n = 19). Conidiomata pycnidial, light brown, opening via central ostiole; wall brown, composed of septate and hyaline hyphae. Conidiophores reduced to conidiogenous cells, lining the inner cavity at the base of the conidioma. Conidiogenous cells ampulliform to subulate, hyaline, smooth, phialidic. Conidia 1-celled, hyaline, ovate to ellipsoidal, thin-walled, smooth, and produced in hyaline slimy mass. Chlamydospores hyaline to dark brown, intercalar or terminal, globose to subglobose.

Isolates (DS334 and DS1613) tested in three different concentrations of NaCl were able to grow only in the absence of NaCl and in the lowest concentration (50 g/L) (SUPPLEMENTARY FIG. 5). All tested isolates possessed cellulolytic and proteolytic activities. However, none of them presented amylolytic activity (SUPPLEMENTARY TABLE 3).

Habitat: Associated with roots of Andropogon gerardii (big bluestem, ANGE), B. dactyloides (buffalo grass, BUDA), B. eriopoda (black grama, BOER), B. gracilis (blue grama, BOGR), and Schizachyrium scoparium (little bluestem, SCSC).

*Distribution:* This species is known from plant roots from 22 sites in the North American Plains of the United States (SUPPLEMENTARY TABLE 1).

**Pleoardoris graminearum** X.J. Pinchi-Davila & A. Porras-Alfaro, sp. nov. FIGS. 6–7; SUPPLEMENTARY FIG. 4 MycoBank MB836053

*Typification:* USA. TEXAS: Guadalupe Mountains National Park, latitude: 31.969083, longitude:

-104.760016, in the roots of *Bouteloua gracilis* (holotype FLAS-F-71013, DS304, dried specimen in metabolically inactive state). GenBank: ITS = MK808676; 28S = MT707514; 18S = MT707488; *ACT* = MT750209; *CAL* = MT733192.

*Etymology*: The epithet refers to the grass family Gramineae, the host plants of this fungus. It is in the genitive plural form that means "of the grasses."

Description: Colonies on MEA 36 mm diam on average after 10 d in the dark at 25 C. Orange-brown (RAL8023) colonies that become darker with age, present radial growth with filamentous margins and sparse flat mycelium. Colonies on PDA 48 mm diam on average after 10 d in the dark at 25 C. Colonies are pearl (RAL1013), present radial growth with filamentous margins and aerial mycelium. Colonies on Czapek-Dox agar 15.4 mm diam on average after 10 d in the dark at 25 C. Colonies are orange-brown (RAL8023) in the center and light ivory (RAL1015) in the margins, present radial growth and sparse flat mycelium. Colonies on DG18 8 mm diam on average after 10 d in the dark at 25 C. Colonies are pearl (RAL1013), have irregular filamentous margins, and grow more aerial mycelium compared with cultures grown on other media. Colonies on OA+A 47.4 mm diam on average after 10 d in the dark at 25 C. Colonies are light ivory (RAL1015), have flat mycelium, and secretes abundant copper brown pigments (RAL8004) into the medium. Colonies become darker with age. Colonies on LA after 14 d in the dark at 25 C are ivory (RAL1014), have flat mycelium, grow slower compared with cultures grown on other media, and secrete pigments that change the color of the medium to signal yellow (RAL1003). Colonies on SA 12.6 mm

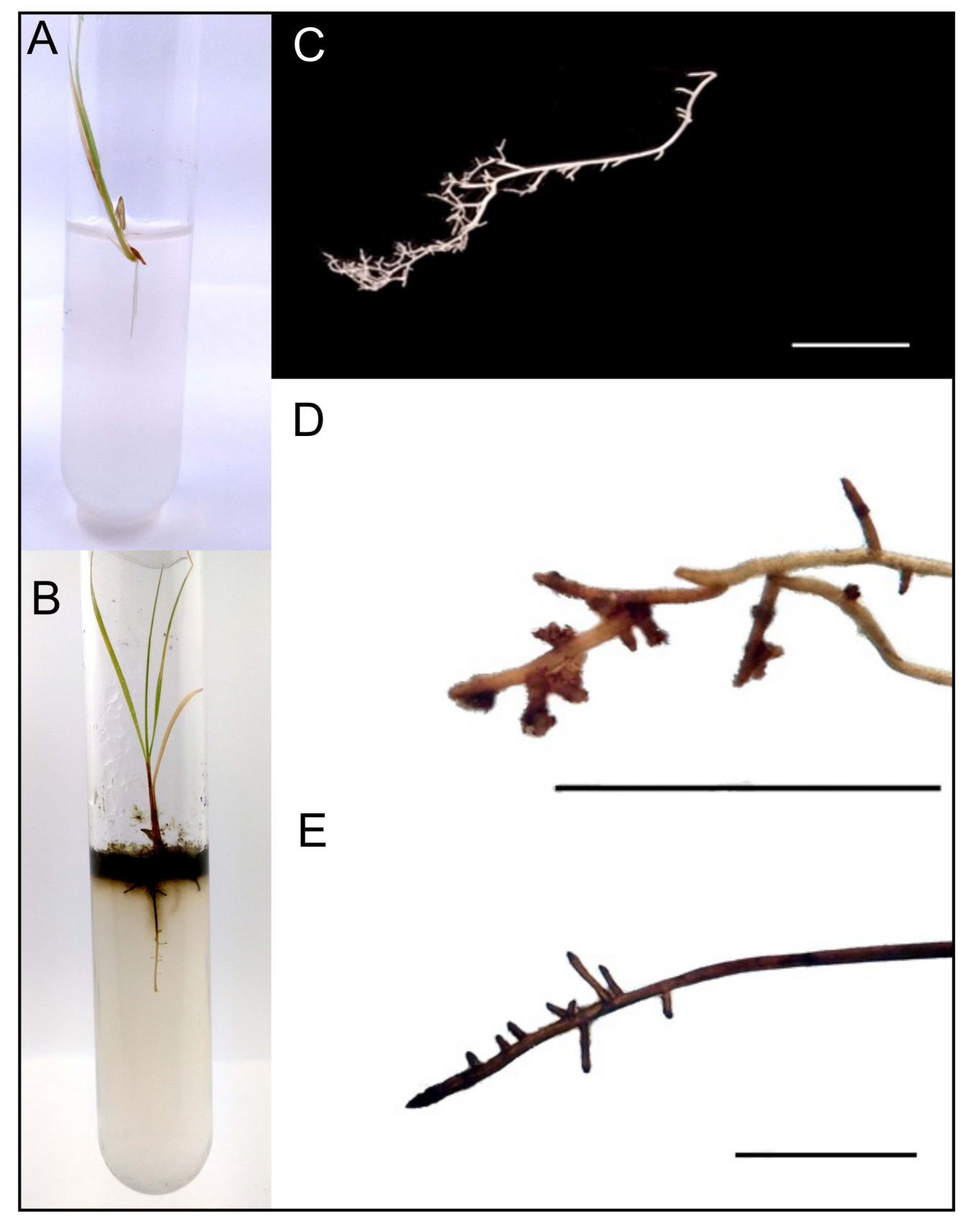


**Figure 5.** Root morphology modification of *B. gracilis* by *P. graminearum*. A. Control (no fungus). B. Plant inoculated with isolate DS304. C. Root of noninoculated seedling. D–E. Roots of inoculated seedlings. Bar = 5 mm.

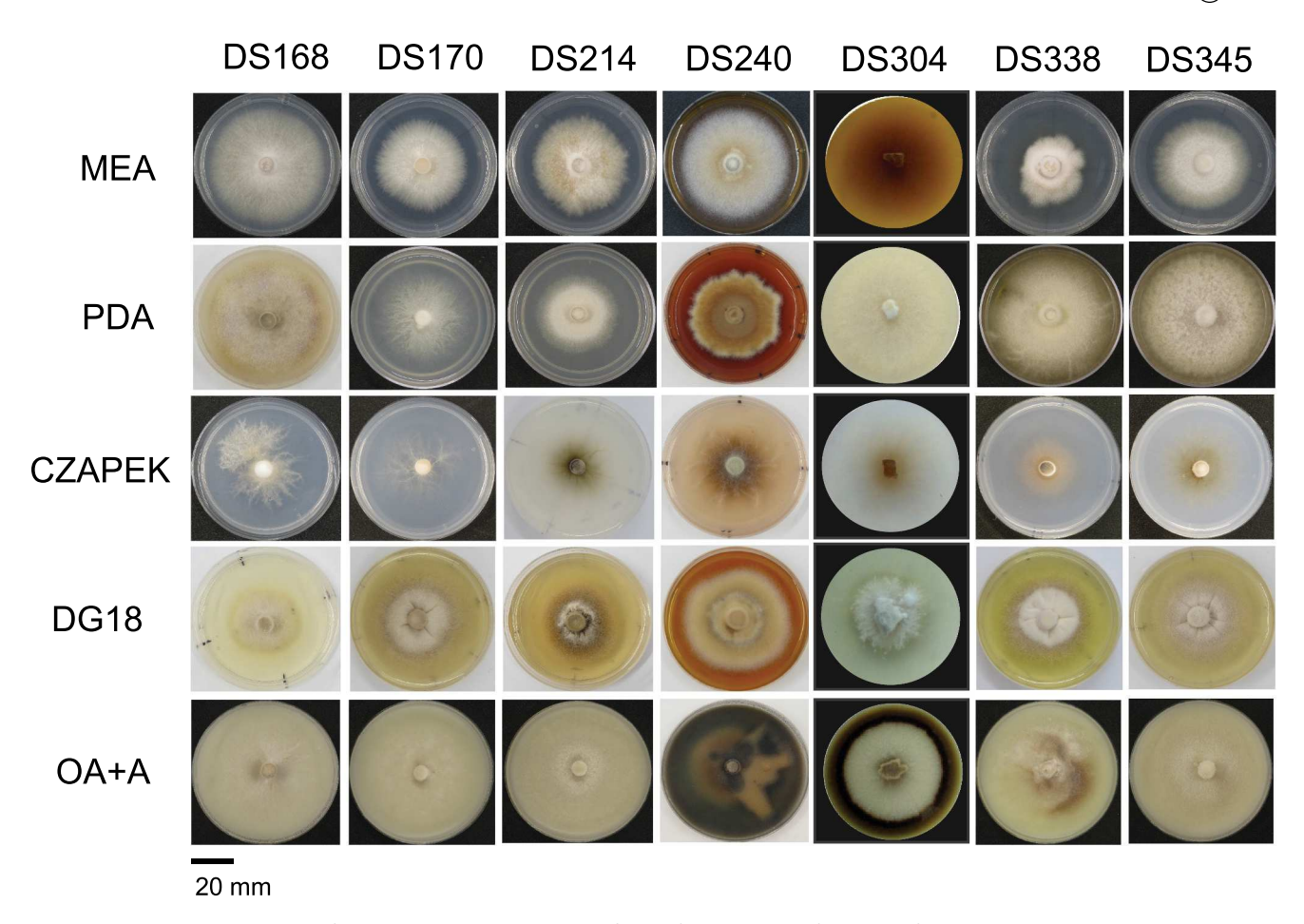


Figure 6. Colony morphology of *Pleoardoris graminearum* on five different media after 14 d of incubation. MEA = malt extract agar; PDA = potato dextrose agar; OA+A = oatmeal agar plus antibiotics; QN+A = quinoa agar plus antibiotics. Bar = 20 mm.

diam on average after 10 d in the dark at 25 C. Colonies are beige gray (RAL7006), present radial growth with irregular filamentous margins and flat mycelium. Colonies on SDA 36.6 mm diam on average after 10 d in the dark at 25 C. Colonies are signal brown (RAL8002) in the center and light ivory (RAL1015) in the margins, present radial growth and flat mycelium. Colonies on MMN 22.6 mm diam on average after 10 d in the dark at 25 C. Colonies are ivory (RAL1014) in the center and light ivory in the margins (RAL1015), have radial growth and flat mycelium. Hyphae are septate, highly branched, multinucleate, cylindrical, and thin-walled,  $0.9-3.3~\mu m$ diam,  $2 \pm 0.6 \,\mu m$  average  $\pm$  SD (n = 30, MEA medium). Sometimes the hyphae are funiculose or form coils. When grown on OA+A, hyphae of young cultures measure 1.2- $2.6 \mu m \text{ diam}$ ,  $1.9 \pm 0.4 \mu m \text{ average} \pm \text{SD (n} = 30)$ . Hyphae of older cultures are wider in diameter, and some cells become swollen, 4.3–13  $\times$  2.3–8.3  $\mu m$  total range, 7.1  $\pm$  $1.9 \times 4.3 \pm 1.3 \,\mu m$  average  $\pm$  SD (n = 30). Hyaline to dark brown intercalar and terminal chlamydospores, globose to subglobose, 6.6–12.7  $\times$  7.7–13.3  $\mu m$  total range, 10.3  $\pm$  $1.4 \times 10.3 \pm 1.4 \,\mu m$  average  $\pm$  SD (n = 30). Some isolates

cultured on QN and KW produced light brown pycnidum-like conidioma with a central ostiole. Pycnidiumlike conidioma wall is made of septate and hyaline hyphae. Conidiogenous cells occurring at the base of the conidioma, phialidic, ampulliform to subulate, 5.8–12.6  $\times$ 1–3.3  $\mu m$  total range, 8.4  $\pm$  1.8  $\times$  2  $\pm$  0.6  $\mu m$  average  $\pm$  SD (n = 30). Conidia are produced in hyaline slimy mass. Conidia 1-celled, hyaline, ovate to ellipsoidal, thin-walled and smooth, 2.7–3.8  $\times$  1.2–2.8  $\mu m$  total range, 3.1  $\pm$  0.2  $\times$  $1.6 \pm 0.2 \,\mu m$  average  $\pm \, SD \, (n = 30)$ .

Isolate DS304 grows only in the lowest concentration (50 g/L) of NaCl or on media without NaCl (SUPPLEMENTARY FIG. 5). The fungus possesses cellulolytic and proteolytic activities but not amylolytic activity (SUPPLEMENTARY TABLE 3).

Habitat: Isolated from roots of B. gracilis plants collected from Guadalupe Mountains National Park (Texas).

Genome sequencing: The genomes for isolates DS304 and DS1613 assembled to over 100 Mb each, at 105.42 and 101.79 Mb, respectively. These sizes are notably larger than other published genomes of dark septate

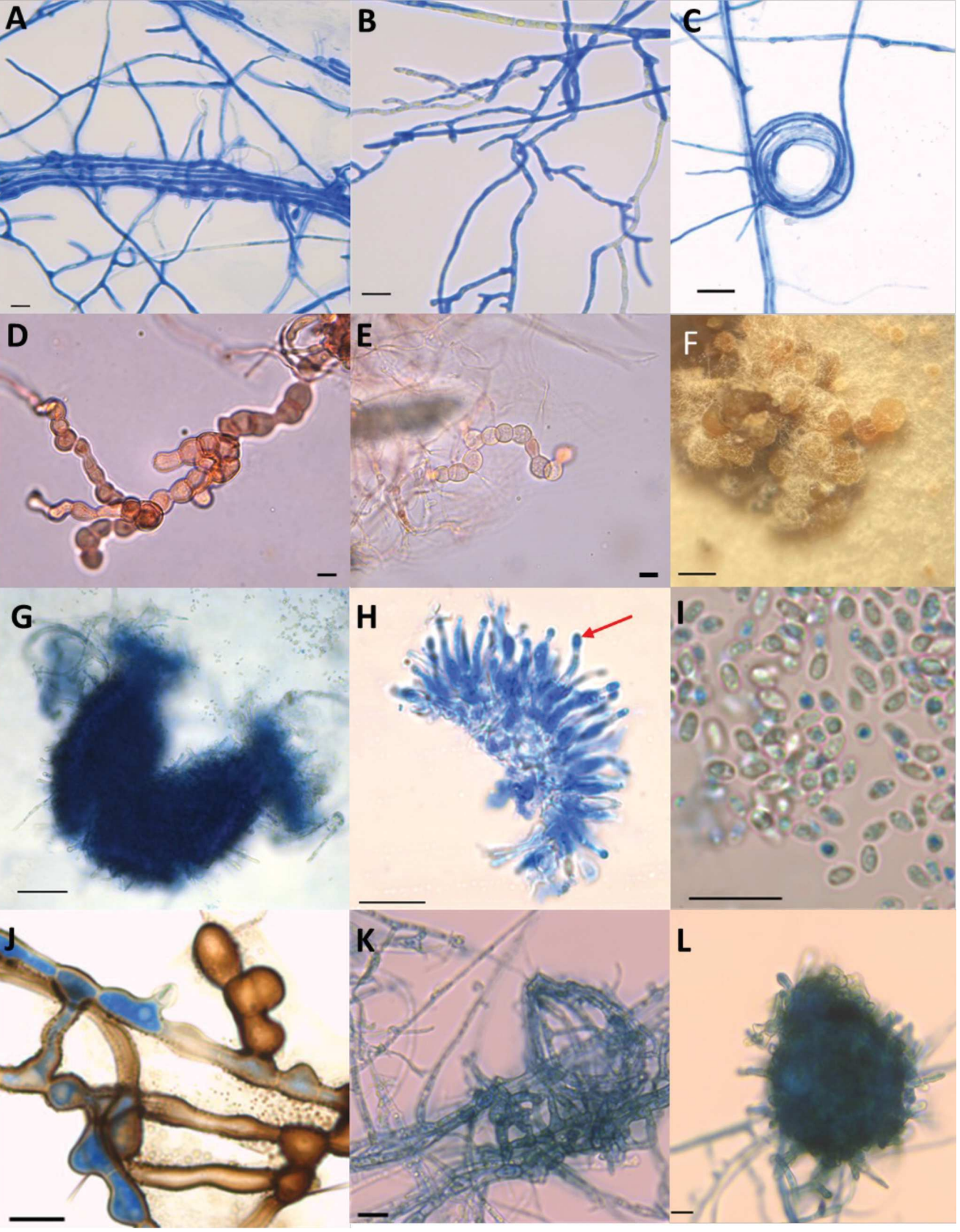


Figure 7. Light microscopy of P. graminearum. A-E. Hyphae morphology, isolate DS304. A. Funiculose hyphae on OA+A. B. Branched, septate, and hyaline hyphae on OA+A. C. Hyphae forming a ring on OA+A. D-E. Chlamydospores. F. Pycnidia on QN+A, isolate DS170. G. Pycnidium on QN+A, isolate DS170. H. Conidiogenous cells on QN+A, isolate DS170. Arrow indicates conidia attached to conidiogenous cells. I. Spores on QN+A, isolate DS187. J. Hyphae containing melanin after 54 d of incubation on PDA, isolate DS170. K. Hyphae forming a pycnidium on QN+A, isolate DS187. L. Pycnidium on early stage of formation on QN+A, isolate DS187. Bars: A,B =  $10 \mu m$ ; C =  $20 \mu m$ ; D,E =  $10 \mu m$ ; F=  $500 \mu m$ ; G=  $50 \mu m$ ; H-L =  $10 \mu m$ .

endophytes in the Pleosporales, such as Periconia macrospinosa, which assembled to 54.99 Mb (Knapp et al. 2018), and Darksidea phi, which assembled to a similar size of 52.3 Mb (Romero-Jiménez et al. 2022). The doubling in genome size observed in *Pleoardoris* graminearum appears to be largely accounted for by AT-rich stretches that contain very few gene regions, as demonstrated by the output from OcculterCut. Furthermore, the *P. graminearum* genomes were relatively low in gene content despite their increased size. Specifically, DS304 and DS1613 contained 13 431 and 13 751 gene models, respectively, counts that are on par with other DSF genomes in the Pleosporales: Periconia macrospinosa (18 750; Knapp et al. 2018) and D. phi (14 707; Romero-Jiménez et al. 2022).

Notes: ITS2 metabarcode data also indicate presence of Pleoardoris graminearum on roots of A. gerardii and S. scoparium and in a wide range of sites (22 of 24 sites sampled). Other potentially representative sequences of this fungus have been detected in soil from India (MH858658), and in B. gracilis from Mexico (GQ923977), as indicated by BLASTn analysis in GenBank (>97% similarity cutoff for the ITS region).

#### **DISCUSSION**

In this study, we combined direct culturing, microscopy, bioassays, field experiments, and next-generation sequencing techniques to fully describe P. graminearum, gen. et sp. nov., a monotypic genus of Pleosporales from the North American Plains. Our phylogenetic, phylogenomic, and sequence similarity analyses showed strong support for the placement of this novel species within the Montagnulaceae family. Morphological differences among our 14 isolates and Didymocrea, Kalmusia, and Bimuria also support its typification as a novel species. Didymocrea sadasivanii was the closest match to P. graminearum based on 28S sequence similarity (98.5%) and showed low similarity for ITS (<72%), supporting P. graminearum as a distinct clade from this genus.

The novel genus Pleoardoris is a dark septate root fungus broadly distributed in West, Midwest, and Southwest grasslands in the United States, as detected using Illumina and also from root isolates. Analysis of Illumina data confirmed a latitudinal gradient of the relative abundance of *P. graminearum* as well as divergent patterns in host plant association. These results support previous evidence that host plant species have strong influence on the environmental correlates of root fungal composition and colonization (Ranelli et al. 2015; Rudgers et al. 2022). Although some studies suggest that edaphic factors surpass the influence of host identity influence on fungal distribution (Bokati et al. 2016; Erlandson et al. 2018; Glynou et al. 2016; Timling et al. 2012), our analysis suggests that host identity was the most important factor that explained variation in the distribution, relative abundance, and drought sensitivity of *P. graminearum*, supporting the results by Rudgers et al. (2022), who reported that host identity was the primary filter of fungal composition in plant roots across a large set of root-associated fungi.

Our multiyear field-based drought experiment revealed a similar host plant filter on the responses of P. graminearum to extreme drought. In five of the six host species, abundance declined under EDGE drought, although the decline was significant only in B. gracilis and B. eriopoda in central New Mexico (site SEV-B). These results were consistent with our laboratory-based drought-osmotic tolerance assays, in which the two isolates tested only grew in the absence of NaCl and in the lowest salt concentration. These findings are also consistent with other reports from the same experimental plots, where soil fungal and bacterial taxonomic richness decreased at the driest location (SEV); moreover, change in the soil fungal communities was directly proportional to the precipitation gradient (Ochoa-Hueso et al. 2018). Studies that have examined the responses of root-associated and nonmycorrhizal fungi to drought suggest that these communities can be strongly affected by drought (Wang et al. 2017). In our broader analysis of the whole fungal community response to drought, plant species identity and site had stronger effects on overall root-associated fungal community composition than drought. Moreover, P. graminearum was identified as an indicator species for host identity; in particular, this species contributed strongly to the unique fungal community associated with B. gracilis (Lagueux et al. 2021).

As suggested by earlier research, DSF can enhance plant growth and survival by increasing water supply and mineral uptake (e.g., through extraradical networks of hyphae), as well as by protecting plants from biotic or abiotic stress (e.g., through production of secondary compounds or antioxidants) (Likar and Regvar 2013; Newsham 2011; Wang et al. 2016). We found variable responses of B. gracilis to P. graminearum in our in vitro experiment, which highlights the complexity of plant-fungal interactions. In contrast to a previous experiment where the inoculation of five different DSF (Pleosporales) decreased B. gracilis dry shoot weight and relative C concentration, our results showed that one *P. graminearum* isolate increased root length up to 34% compared with controls (Perez-Naranjo 2009). Other reports also indicated that DSF can colonize several hosts, and their effect on plant

growth can vary from positive to negative (Herrera et al. 2010; Jumpponen and Trappe 1998; Mandyam and Jumpponen 2005). For example, Ammopiptanthus mongolicus, an endemic forb of eastern desert of Central Asia, inoculated with strains of DSF representing two genera (Paraconiothyrium and Darksidea) and grown under drought stress had shorter shoots and accumulated less biomass compared with controls (Li et al. 2018). In contrast, when inoculated with Phialophora graminicola, a dark septate endophyte, the grass Vulpia ciliata ssp. ambigua, had longer roots and higher shoot, root, and total biomass values compared with noninoculated plants (Newsham 1999). DSF not only can increase root length but can also alter root morphology as shown in our results, where fungus-free plants inoculated with P. graminearum isolates developed thicker and dark-pigmented roots compared with controls. The modification of roots by DSF has been reported in both beneficial and pathogenic interactions. For instance, Acrocalymma vagum, a DSF, can modify root morphology and ultrastructure, increase the number of vacuoles, and balance endogenous root hormones to improve Ormosia hosiei tolerance to drought (Liu and Wei 2019). Conversely, when Ascochyta medicaginicola (= Phoma medicaginis), another DSF, interacted with Medicago sativa, it reduced shoot and root development (Djebali 2013). Our results demonstrate that DSF forms symbiotic interactions with host plants; however, the nature of these interactions vary across isolates.

Volatile organic compounds (VOCs) produced by fungi can promote plant growth and enhance disease resistance (Lee et al. 2015; Naznin et al. 2013, 2014; Yamagiwa et al. 2011), and our results showed that P. graminearum isolates benefited B. gracilis growth by increasing both root and stem lengths when grown in proximity to the plant. This finding is consistent with reports for Cladosporium and Phoma, which have been reported to positively influence Arabidopsis thaliana and tobacco plants, respectively (Naznin et al. 2013, 2014). However, the strong positive effect of P. graminearum isolates on B. gracilis stem and root lengths could also be the result of increased CO<sub>2</sub> due to fungal respiration in a closed and aseptic system, which allowed the host plant to become more productive and potentially increase its photosynthetic rate by losing less water from open stomata. Additional tests would be necessary to determine the specific mechanism of interaction between B. gracilis and P. graminearum.

Description of this new taxon exemplifies the potential of using a combination of culture-based and cultureindependent methods to discover and report the

potential ecological roles of previously undescribed dark septate root endophytes.

#### **ACKNOWLEDGMENTS**

Isolation of Pleoardoris cultures was possible due to sampling efforts and processing by Anny Chung, Terri Billingsley Tobias, Terry Torres-Cruz, Cedric Ndinga-Muniania, Paris Salazar-Hamm, Shane Mason, and Adevemi Olanrewaju. The authors would like to thank Aaron Jon Robinson for his support in the genome analysis as well as past and current members of the Fungal Ecology Laboratory at Western Illinois University for the help provided to process the samples.

#### **DISCLOSURE STATEMENT**

No potential conflict of interest was reported by the author(s).

#### **FUNDING**

The research presented in this paper was supported by NSF-DEB no. 1457309 to Dr. Jumpponen, no. 1619935 to Dr. Herrera, no. 1457002 to Dr. Porras-Alfaro, and no. 1456955 to Dr. Rudgers, and by the U.S. Department of Energy (DOE) Biological and Environmental Research Division through Science Focus Area grants to Dr. Dunbar [F255LANL2018] and Dr. Cheryl Kuske [F260LANL2013]. This material is based upon work supported by the National Science Foundation (A.P.-A.). Any opinion, findings, and conclusions or recommendations expressed in this material are those of the author(s) and do not necessarily reflect the views of the National Science Foundation.

#### **ORCID**

Xiomy-Janiria Pinchi-Davila http://orcid.org/0000-0002-6780-1748

#### LITERATURE CITED

Albright MBN, Johansen R, Lopez D, Gallegos-Graves LV, Steven B, Kuske CR, Dunbar J. 2018. Short-term transcriptional response of microbial communities to nitrogen fertilization in a pine forest soil. Appl Environ Microbiol. 84: e00598-18. doi:10.1128/AEM.00598-18.

Bankevich A, Nurk S, Antipov D, Gurevich AA, Dvorkin M, Kulikov AS, Lesin VM, Nikolenko SI, Pham S, Prjibelski AD, et al. 2012. SPAdes: a new genome assembly algorithm and its applications to single-cell sequencing. J Comput Biol. 19:455-477. doi:10.1089/cmb.2012.0021.

Barton K. 2019. Mu-Min: multi-model inference. R-package Version. 1:43.15.

Becker SR, Byrne PF, Reid SD, Bauerle WL, McKay JK, Haley SD. 2016. Root traits contributing to drought tolerance of synthetic hexaploid wheat in a greenhouse study. Euphytica. 207:213-224. doi:10.1007/s10681-015-1574-1.

Berthelot C, Leyval C, Foulon J, Chalot M, Blaudez D. 2016. Plant growth promotion, metabolite production and metal



- tolerance of dark septate endophytes isolated from metalpolluted poplar phytomanagement sites. FEMS Microbiol Ecol. 92:144. doi:10.1093/femsec/fiw144.
- Bokati D, Herrera J, Poudel R. 2016. Soil influences colonization of root-associated fungal endophyte communities of maize, wheat, and their progenitors. J Mycol. 2016:1-9. doi:10.1155/2016/8062073.
- Bushnell B, Rood J, Singer E. 2017. BBMerge accurate paired shotgun read merging via overlap. PLOS ONE. 12: e0185056. doi:10.1371/journal.pone.0185056.
- Bustamante Gonzales SR. 2018. Evaluación del potencial antifúngico de los extractos etanólicos de Phyllanthus niruri y Minthostachys mollis frente al hongo Botrytis cinerea [Bachelor's Thesis]. Lima (Peru): Universidad Nacional Mayor de San Marcos.
- Carbone I, Kohn LM. 1999. A method for designing primer sets for speciation studies in filamentous ascomycetes. Mycologia. 91:553-556. doi:10.1080/00275514.1999. 12061051.
- Dayton PK. 1972. Toward an understanding of community resilience and the potential effects of enrichments to the Benthos at McMurdo sound, Antarctica. Scripps Institution of Oceanography, La Jolla Cali. f. p. 17.
- Djebali N. 2013. Aggressiveness and host range of Phoma medicaginis isolated from Medicago species growing in Tunisia. Phytopathol Mediterr. 52:3-15.
- Ellison AM, Bank MS, Clinton BD, Colburn EA, Elliott K, Ford CR, Foster DR, Kloeppel BD, Knoepp JD, Lovett GM, et al. 2005. Loss of foundation species: consequences for the structure and dynamics of forested ecosystems. Front Ecol Environ. 3:479-486. doi:10.1890/1540-9295(2005)003 [0479:LOFSCF]2.0.CO;2.
- Emery SM, Rudgers JA. 2013. Impacts of simulated climate change and fungal symbionts on survival and growth of a foundation species in sand dunes. Oecologia. 173:1601-12. doi:10.1007/s00442-013-2705-9.
- Erlandson S, Wei X, Savage J, Cavender-Bares J, Peay K. 2018. Soil abiotic variables are more important than Salicaceae phylogeny or habitat specialization in determining soil microbial community structure. Mol Ecol. 27:2007-2024. doi:10.1111/mec.14576.
- Gardes M, Bruns TD. 1993. ITS primers with enhanced specificity for basidiomycetes-application to the identification of mycorrhizae and rusts. Mol Ecol. 2:113-118. doi:10. 1111/j.1365-294X.1993.tb00005.x.
- Gihring TM, Green SJ, Schadt CW. 2012. Massively parallel rRNA gene sequencing exacerbates the potential for biased community diversity comparisons due to variable library sizes. Environ Microbiol. 14:285-290. doi:10.1111/j.1462-2920.2011.02550.x.
- Glass NL, Donaldson GC. 1995. Development of primer sets designed for use with the PCR to amplify conserved genes from filamentous ascomycetes. Appl Environ Microbiol. 61:1323-1330. doi:10.1128/aem.61.4.1323-1330.1995.
- Glynou K, Ali T, Buch A-K, Haghi Kia S, Ploch S, Xia X, Çelik A, Thines M, Maciá-Vicente JG. 2016. The local environment determines the assembly of root endophytic fungi at a continental scale. Environ Microbiol. 18:2418-2434. doi:10. 1111/1462-2920.13112.
- Groenewald JZ, Nakashima C, Nishikawa J, Shin H-D, Park J-H, Jama AN, Groenewald M, Braun U, Crous PW. 2013.

- Species concepts in Cercospora: spotting the weeds among the roses. Stud Mycol. 75:115-170. doi:10.3114/sim0012.
- Gurevich A, Saveliev V, Vyahhi N, Tesler G. 2013. QUAST: quality assessment tool for genome assemblies. Bioinformatics. 29:1072-1075. doi:10.1093/bioinformatics/ btt086.
- Herrera J, Khidir HH, Eudy DM, Porras-Alfaro A, Natvig DO, Sinsabaugh RL. 2010. Shifting fungal endophyte communities colonize Bouteloua gracilis: effect of host tissue and geographical distribution. Mycologia. 102:1012-1026. doi:10.3852/09-264.
- Hung R, Lee S, Bennett JW. 2013. Arabidopsis thaliana as a model system for testing the effect of Trichoderma volatile organic compounds. Fungal Ecol. 6:19-26. doi:10.1016/j. funeco.2012.09.005.
- Ihrmark K, Bödeker ITM, Cruz-Martinez K, Friberg H, Kubartova A, Schenck J, Strid Y, Stenlid J, Brandström-Durling M, Clemmensen KE, et al. 2012. New primers to amplify the fungal ITS2 region - evaluation by 454-sequencing of artificial and natural communities. FEMS Microbiol Ecol. 82:666–677. doi:10.1111/j.1574-6941.2012.01437.x.
- Jumpponen A. 2001. Dark septate endophytes Are they mycorrhizal? Mycorrhiza. 11:207-211. doi:10.1007/ s005720100112.
- Jumpponen A, Herrera J, Porras-Alfaro A, Rudgers J. 2017. Biogeography of root-associated endophytes. In: Tedersoo L, editor. Biogeography of Mycorrhizal Symbiosis. Tartu (Estonia): Springer Nature; p. 195-222.
- Jumpponen A, Trappe JM. 1998. Dark septate endophytes: a review of facultative biotrophic root-colonizing fungi. New Phytol. 140:295-310. doi:10.1046/j.1469-8137.1998. 00265.x.
- Kahle D, Wickham H. 2013. ggmap: spatial visualization with ggplot2. R J. 5:144. doi:10.32614/RJ-2013-014.
- Katoh K, Standley DM. 2013. MAFFT multiple sequence alignment software version 7: improvements in performance and usability. Mol Biol Evol. 30:772-780. doi:10. 1093/molbev/mst010.
- Kivlin SN, Emery SM, Rudgers JA. 2013. Fungal symbionts alter plant responses to global change. Am J Bot. 100:1445-1457. doi:10.3732/ajb.1200558.
- Knapp DG, Kovács GM, Zajta E, Groenewald JZ, Crous PW. 2015. Dark septate endophytic pleosporalean genera from semiarid areas. Persoonia. 35:87-100.
- Knapp DG, Németh JB, Barry K, Hainaut M, Henrissat B, Johnson J, Kuo A, Lim JHP, Lipzen A, Nolan M, et al. 2018. Comparative genomics provides insights into the lifestyle and reveals functional heterogeneity of dark septate endophytic fungi. Sci Rep. 8(1):6321. doi:10.1038/s41598-018-24686-4.
- Knapp DG, Pintye A, Kovács GM. 2012. The dark side is not fastidious - Dark septate endophytic fungi of native and invasive plants of semiarid sandy areas. PLOS ONE. 7(2): e32570. doi:10.1371/journal.pone.0032570.
- Lagueux D, Jumpponen A, Porras-Alfaro A, Herrera J, Chung YA, Baur LE, Smith MD, Knapp AK, Collins SL, Rudgers JA. 2021. Experimental drought re-ordered assemblages of root-associated fungi across North American grasslands. J Ecol. 109(2):776–792. doi:10.1111/1365-2745.13505.
- Leach CM. 1962. Sporulation of diverse species of fungi under near-ultraviolet radiation. Canad J Bot. 40(1):151-161. doi:10.1139/b62-016.



- Lee S, Hung R, Yap M, Bennett JW. 2015. Age matters: the effects of volatile organic compounds emitted by *Trichoderma atroviride* on plant growth. Arch Microbiol. 197(5):723–727. doi:10.1007/s00203-015-1104-5.
- Lefcheck J. 2016. piecewiseSEM: piecewise structural equation modelling in r for ecology, evolution, and systematics. Methods Ecol Evol. 7(5):573–579. doi:10.1111/2041-210X. 12512.
- Li X, He X, Hou L, Ren Y, Wang S, Su F. 2018. Dark septate endophytes isolated from a xerophyte plant promote the growth of *Ammopiptanthus mongolicus* under drought condition. Sci Rep. 8(1):7896. doi:10.1038/s41598-018-26183-0.
- Likar M, Regvar M. 2013. Isolates of dark septate endophytes reduce metal uptake and improve physiology of Salix caprea L. Plant Soil. 370(1–2):593–604. doi:10.1007/s11104-013-1656-6.
- Liu Y, Wei X. 2019. Dark septate endophyte improves drought tolerance of *Ormosia hosiei* Hemsley & E. H. Wilson by modulating root morphology, ultrastructure, and the ratio of root hormones. Forests. 10:830.
- Love J, Palmer J, Stajich J, Esser T, Kastman E, Winter D. 2018. nextgenusfs/funannotate: funannotate v1.5.1. Zenodo.
- Mandyam K, Jumpponen A. 2005. Seeking the elusive function of the root-colonising dark septate endophytic fungi. Stud Mycol. 53:173–189. doi:10.3114/sim.53.1.173.
- Masson-Delmotte V, Pörtner H-O, Skea J, Zhai P, Roberts D, Shukla PR, Pirani A, Pidcock R, Chen Y, Lonnoy E, et al. 2018. An IPCC special report on the impacts of global warming of 1.5°C above pre-industrial levels and related global greenhouse gas emission pathways, in the context of strengthening the global response to the threat of climate change, sustainable development, and efforts to eradicate poverty.
- Mueller GM, Bills GF, Foster MS, editors. 2004. Biodiversity of fungi: inventory and monitoring methods. San Diego (CA): Elsevier Academic Press.
- Mueller RC, Gallegos-Graves LV, Kuske CR. 2016. A new fungal large subunit ribosomal RNA primer for high-throughput sequencing surveys. FEMS Microbiol Ecol. 92 (2):153.
- Naznin HA, Kimura M, Miyazawa M, Hyakumachi M. 2013. Analysis of volatile organic compounds emitted by plant growth-promoting Fungus *Phoma* sp. GS8-3 for growth promotion effects on tobacco. Microbes Environ. 28: (1):42–49. doi:10.1264/jsme2.ME12085.
- Naznin HA, Kiyohara D, Kimura M, Miyazawa M, Shimizu M, Hyakumachi M. 2014. Systemic resistance induced by volatile organic compounds emitted by plant growth-promoting fungi in *Arabidopsis thaliana*. PLOS ONE. 9(1): e86882. doi:10.1371/journal.pone.0086882.
- Ndinga-Muniania C, Mueller RC, Kuske CR, Porras-Alfaro A. 2021. Seasonal variation and potential roles of dark septate fungi in an arid grassland. Mycologia. 113(6):1181–1198. doi:10.1080/00275514.2021.1965852.
- Newsham KK. 1999. Phialophora graminicola, a dark septate fungus, is a beneficial associate of the grass Vulpia ciliata ssp. ambigua. New Phytol. 144:(3):517–524. doi:10.1046/j. 1469-8137.1999.00537.x.
- Newsham KK. 2011. A meta-analysis of plant responses to dark septate root endophytes. New Phytol. 190(3):783–793. doi:10.1111/j.1469-8137.2010.03611.x.

- Ochoa-Hueso R, Collins SL, Delgado-Baquerizo M, Hamonts K, Pockman WT, Sinsabaugh RL, Smith MD, Knapp AK, Power SA. 2018. Drought consistently alters the composition of soil fungal and bacterial communities in grasslands from two continents. Glob Chang Biol. 24(7):2818–2827. doi:10.1111/gcb.14113.
- Paul D, Park KS. 2013. Identification of Volatiles Produced by *Cladosporium cladosporioides* CL-1, a Fungal Biocontrol Agent That Promotes Plant Growth. Sensors. 13(10):13969–13977. doi:10.3390/s131013969.
- Perez-Naranjo JC. 2009. Dark septate and arbuscular mycorrhizal fungal endophytes in roots of prairie grasses [Dissertation]. Saskatoon (CA): University of Saskatchewan.
- Porras-Alfaro A, Herrera J, Sinsabaugh RL, Odenbach KJ, Lowrey T, Natvig DO. 2008. Novel root fungal consortium associated with a dominant desert grass. Appl Environ Microbiol. 74(9):2805–2813. doi:10.1128/AEM.02769-07.
- Quaedvlieg W, Kema GHJ, Groenewald JZ, Verkley GJM, Seifbarghi S, Razavi M, Mirzadi Gohari A, Mehrabi R, Crous PW. 2011. *Zymoseptoria* gen. nov: a new genus to accommodate Septoria-like species occurring on graminicolous hosts. Persoonia. 26:57–69.
- Rambaut A, Drummond AJ. 2012. FigTree version 1.4.4.
- Ranelli LB, Hendricks WQ, Lynn JS, Kivlin SN, Rudgers JA. 2015. Biotic and abiotic predictors of fungal colonization in grasses of the Colorado Rockies. Divers Distrib. 21(8):962–976. doi:10.1111/ddi.12310.
- Rehner SA, Samuels GJ. 1994. Taxonomy and phylogeny of *Gliocladium* analysed from nuclear large subunit ribosomal DNA sequences. Mycol Res. 98(6):625–634. doi:10.1016/S0953-7562(09)80409-7.
- Riddell RW. 1950. Permanent Stained Mycological Preparations Obtained by Slide Culture. Mycologia. 42 (2):265–270. doi:10.1080/00275514.1950.12017830.
- Rodriguez RJ, White JF Jr, Arnold AE, Redman RS. 2009. Fungal endophytes: diversity and functional roles. New Phytol. 182(2):314–330. doi:10.1111/j.1469-8137.2009. 02773.x.
- Romero-Jiménez M-J, Rudgers JA, Jumpponen A, Herrera J, Hutchinson M, Kuske C, Dunbar J, Knapp DG, Kovács GM, Porras-Alfaro A. 2022. *Darksidea phi*, sp. nov., a dark septate root-associated fungus in foundation grasses in North American great plains. Mycologia. 114:(2):254–269. doi:10.1080/00275514.2022.2031780.
- Rudgers JA, Fox S, Porras-Alfaro A, Herrera J, Reazin C, Kent DR, Souza L, Chung YA, Jumpponen A. 2022. Biogeography of root-associated fungi in foundation grasses of North American plains. Biogeography. 49 (1):22–37. doi:10.1111/jbi.14260.
- Santos M, Cesanelli I, Diánez F, Sánchez-Montesinos B, Moreno-Gavíra A. 2021. Advances in the role of dark septate endophytes in the plant resistance to abiotic and biotic stresses. J Fungi. 7(11):939. doi:10.3390/jof7110939.
- Schulz-Bohm K, Martín-Sánchez L, Garbeva P. 2017. microbial volatiles: small molecules with an important role in intra- and inter-kingdom interactions. Front Microbiol. 8:8. doi:10.3389/fmicb.2017.00008.
- Simão FA, Waterhouse RM, Ioannidis P, Kriventseva EV, Zdobnov EM. 2015. BUSCO: assessing genome assembly and annotation completeness with single-copy orthologs. Bioinformatics. 31(19):3210–3212. doi:10.1093/bioinformatics/btv351.



- Stajich JE, Palmer JM. 2018. Automatic assembly for the fungi. Stamatakis A. 2014. RAxML version 8: a tool for phylogenetic analysis and post-analysis of large phylogenies. Bioinformatics. 30(9):1312-1313. doi:10.1093/bioinformatics/btu033.
- Stanke M, Steinkamp R, Waack S, Morgenstern B. 2004. AUGUSTUS: a web server for gene finding in eukaryotes. Nucleic Acids Res. 32:W309-312. doi:10.1093/nar/gkh379.
- Tamayo-Londoño DM. 2017. Papel de hongos endófitos septados oscuros en la tolerancia del pasto Brachiaria decumbens Stapf a condiciones ambientales extremas de sequía y baja fertilidad general del suelo [Master Thesis]. Medellin (CO): Universidad Nacional de Colombia.
- Tamura K, Stecher G, Kumar S. 2021. MEGA11: molecular evolutionary genetics analysis version 11. Mol Biol Evol. 38 (7):3022-3027. doi:10.1093/molbev/msab120.
- Ter-Hovhannisyan V, Lomsadze A, Chernoff YO, Borodovsky M. 2008. Gene prediction in novel fungal genomes using an ab initio algorithm with unsupervised training. Genome Res. 18(12):1979-1990. doi:10.1101/gr.081612.108.
- Testa AC, Oliver RP, Hane JK. 2016. OcculterCut: a comprehensive survey of at-rich regions in fungal genomes. Genome Biol Evol. 8(6):2044-2064. doi:10.1093/gbe/evw 121.
- Thomson JA, Burkholder DA, Heithaus MR, Fourqurean JW, Fraser MW, Statton J, Kendrick GA. 2015. Extreme temperatures, foundation species, and abrupt ecosystem change: an example from an iconic seagrass ecosystem. Glob Chang Biol. 21(4):1463–1474. doi:10.1111/gcb.12694.
- Timling I, Dahlberg A, Walker DA, Gardes M, Charcosset JY, Welker JM, Taylor DL. 2012. Distribution and drivers of ectomycorrhizal fungal communities across the North American Arctic. Ecosphere 3: 111.
- Torres-Cruz TJ, Billingsley Tobias TL, Almatruk M, Hesse CN, Kuske CR, Desirò A, Benucci GMN, Bonito G, Stajich JE, Dunlap C, et al. 2017. Bifiguratus adelaidae, gen. et sp. nov., a new member of Mucoromycotina in endophytic and soil-dwelling habitats. Mycologia. 109 (3):363-378. doi:10.1080/00275514.2017.1364958.
- Vilgalys R, Hester M. 1990. Rapid genetic identification and mapping of enzymatically amplified ribosomal DNA from several Cryptococcus species. J Bacteriol. 172(8):4238-4246. doi:10.1128/jb.172.8.4238-4246.1990.

- Vu D, Groenewald M, de Vries M, Gehrmann T, Stielow B, Eberhardt U, Al-Hatmi A, Groenewald JZ, Cardinali G, Houbraken J, et al. 2019. Large-scale generation and analysis of filamentous fungal DNA barcodes boosts coverage for kingdom fungi and reveals thresholds for fungal species and higher taxon delimitation. Stud Mycol. 92(1):135-154. doi:10.1016/j.simyco.2018.05.001.
- Walker BJ, Abeel T, Shea T, Priest M, Abouelliel A, Sakthikumar S, Cuomo CA, Zeng Q, Wortman J, Young SK, et al. 2014. Pilon: an integrated tool for comprehensive microbial variant detection and genome assembly improvement. PloS One. 9(11):e112963. doi:10.1371/journal.pone. 0112963.
- Wang J, Li T, Liu G, Smith JM, Zhao Z. 2016. Unraveling the role of dark septate endophyte (DSE) colonizing maize (Zea mays) under cadmium stress: physiological, cytological and genic aspects. Sci Rep. 6(1):22028. doi:10.1038/srep22028.
- Wang J, Wang Y, Song X, Wang Y, Lei X. 2017. Elevated atmospheric co2 and drought affect soil microbial community and functional diversity associated with Glycine max. Revista Brasileira de Ciência Do Solo. 41:e0160460. doi:10. 1590/18069657rbcs20160460.
- White TJ, Bruns T, Lee S, Taylor JW. 1990. Amplification and direct sequencing of fungal ribosomal RNA genes for phylogenetics. In: Innis MA, Gelfand DH, Sninsky JJ, White TJ, editors. PCR protocols: a guide to the methods and applications. New York: Academic Press. p. 315-322.
- Wickham H. 2016. ggplot 2: elegant graphics for data analysis. New York: Springer-Verlag.
- Woodward C, Hansen L, Beckwith F, Redman RS, Rodriguez RJ. 2012. Symbiogenics: an epigenetic approach to mitigating impacts of climate change on plants. HortScience. 47 (6):699-703. doi:10.21273/HORTSCI.47.6.699.
- Yamagiwa Y, Inagaki Y, Ichinose Y, Toyoda K, Hyakumachi M, Shiraishi T. 2011. *Talaromyces wortmannii* FS2 emits βcaryphyllene, which promotes plant growth and induces resistance. J Gen Plant Pathol. 77(6):336-341. doi:10. 1007/s10327-011-0340-z.
- Zhang Q, Gong M, Yuan J, Hou Y, Zhang H, Wang Y, Hou X. 2017. Dark septate endophyte improves drought tolerance in sorghum. Int J Agric Biol. 19(1):53-60. doi:10.17957/ IJAB/15.0241.